Int. J. Heat Mass Transfer. Vol. 32, No. 12, pp. 2475–2483, 1989
Printed in Great Britain

0017–9310/89 $3.00 + 0.00

Heat transfer enhancement in Rayleigh–Benard convection

J. ANDRZEJ DOMARADZKI
Department of Aerospace Engineering, University of Southern California, Los Angeles, CA 90089-1191, U.S.A.

(*Received* 8 *September* 1988 *and in final form* 10 *April* 1989)

Abstract—Direct numerical simulations of three-dimensional Rayleigh–Benard convection are performed with non-uniform temperature boundary conditions at the lower plate. The boundary conditions excite convective states in a form of counterrotating convective rolls that remain stable for at least ten eddy-turnover times even if their size is significantly different from the size of rolls encountered in natural convection at the same Rayleigh number. For longer times applied temperature forcing becomes ineffective and forced convective patterns lose their stability. Changing the size of the convective elements increases heat transfer by about 15–20% as compared with the case of natural convection.

1. INTRODUCTION

IN RAYLEIGH–BENARD convection for Rayleigh numbers below 10^6 heat is transferred mostly by the action of large-scale convective structures. For low Rayleigh numbers in convection between two rigid plates these structures have a form of well organized, steady, parallel rolls. For higher Rayleigh numbers, the rolls become unstable and convection becomes progressively more complex in both space and time. However, Willis and Deardorff [1] infer from their experiments that the large-scale structures retain their identity even for Rayleigh numbers as high as 1.5×10^6.

The importance of the large-scale structures in determining convective heat transfer for lower Rayleigh numbers is seen in the dependence of the Nusselt number on the wavelength of the convective rolls (horizontal roll size). Two-dimensional numerical simulations of convection with fixed wavelength independent of the Rayleigh number predict heat transfer substantially higher than observed experimentally [2, 3]. This discrepancy between simulations and experiments is caused by the assumption of a fixed wavelength of rolls in the simulations which is contrary to the increase in the roll diameter for the increased Rayleigh numbers observed in experiments [4]. Two-dimensional simulations which take into account the effect of a wavelength variation with the Rayleigh number predict heat transfer in good agreement with experimental results [2–4] for $Ra \lesssim 2 \times 10^4$ but they again overestimate heat transfer for higher Rayleigh numbers [3]. This last effect is caused by the presence of substantial three-dimensional effects at these Rayleigh numbers that cannot be accounted for by the two-dimensional simulations. Fully three-dimensional simulations [5–8] are in good agreement with the experiments for an extensive range of Rayleigh numbers so long as the lateral size of the computational domain is set to the natural (experimental) wavelength of convection at a given Rayleigh number.

Such results suggest that heat transfer at a given Rayleigh number will be generally increased if a wavelength of convective eddies and three-dimensionality of the flow are decreased. Indeed, three-dimensional numerical simulations of convection with shear by Hathaway and Somerville [9] and by Domaradzki and Metcalfe [8] show that one of the effects of shear at moderate Rayleigh numbers ($\lesssim 5 \times 10^4$) is to increase the level of organization of convection by forcing it to be quasi two-dimensional with the convective structures in a form of rolls aligned in the direction of the mean velocity. This results in a slight increase in the Nusselt number over the case without shear. On the other hand, at higher Rayleigh numbers ($Ra = 150\,000$), the action of shear is to increase three-dimensionality of the flow with the resulting decrease in the heat flux [8].

The above results suggest the possibility of controlling heat flux if a method can be devised by which the size and the level of three-dimensionality of the convective structures could be influenced. It is an experimentally established fact that convection may be forced to develop patterns with wavelengths different from those occurring naturally at a given Rayleigh number. For instance, in the experiments of Chen and Whitehead [10] and Busse and Whitehead [11] convection rolls with wavelengths significantly different from the natural one were established by a small temperature perturbation with the prescribed wavelength. More recently convection with forcing was also investigated experimentally by Lowe *et al.* [12]. These authors were able to force rolls with wavelengths in the range 0.8–1.2 times the natural wavelength with very small forcing amplitudes. In the

NOMENCLATURE

A	amplitude of forcing	T_0	temperature of the lower plate
d	distance between plates	ΔT	temperature difference between plates
$\mathbf{g}$	gravitational acceleration	T_n	Chebyshev polynomial of order n
k_c	critical wave number	$\mathbf{u}$	velocity field.
k_y	wave number of forcing		
L_x	periodicity length in the x-direction		
L_y	periodicity length in the y-direction		
n	number of forced rolls		
Nu	Nusselt number	Greek symbols	
P	pressure	α	coefficient of thermal expansion
Pr	Prandtl number	κ	coefficient of thermal diffusivity
Ra	Rayleigh number	ν	coefficient of kinematic viscosity
T	temperature	π	pressure head
$\underset{\sim}{T}$	departure from the linear temperature profile	ρ	reference density
		ω	vorticity field.

above papers heat transfer was not a primary subject of investigation and information about possible influence of roll size on Nusselt number was not provided.

In this paper, we present results of three-dimensional numerical simulations of convection for two different Rayleigh numbers, $Ra = 9000$ and 35 840, where we attempt to control convective structures by temperature boundary conditions at the lower plate. We are interested in forcing convective patterns that result in a significant increase in the heat flux. It is shown that it is possible to change the size of the convective structures and by this, the heat flux may be increased by 15–20% compared with the natural convection. However, the particular forcing chosen in this paper is not effective for times longer than about ten large eddy-turnover times and after such times forced patterns may become unstable. Other methods of forcing that could stabilize convective patterns for longer times are suggested in Section 5.

2. EQUATIONS OF MOTION AND NUMERICAL METHOD

The convection between two rigid parallel plates is governed by the following standard set of hydrodynamic equations with the Boussinesq–Oberbeck approximation:

$$\partial_t \mathbf{u} = \mathbf{u}\times\boldsymbol{\omega} - \alpha \underset{\sim}{T}\mathbf{g} - \nabla\pi + \nu\nabla^2\mathbf{u} \tag{1a}$$

$$\partial_t T = -\nabla\cdot(\mathbf{u}T) + \kappa\nabla^2 T \tag{1b}$$

$$\nabla\cdot\mathbf{u} = 0 \tag{1c}$$

where $\mathbf{u}(x,y,z,t) = (u,v,w)$ is the velocity field, $T(x,y,z,t)$ the temperature field, and $\underset{\sim}{T}$ the departure from the linear temperature profile

$$T(x,y,z,t) = \left\{T_0 - \frac{\Delta T}{d}\left(z - \frac{1}{2}d\right)\right\} + \underset{\sim}{T}(x,y,z,t) \tag{2}$$

where it is assumed that the plates are separated by a distance d and there is a mean positive temperature difference ΔT between the plates. Equations (1a)–(1c) are written in the velocity–vorticity formulation with the vorticity $\boldsymbol{\omega} = \nabla\times\mathbf{u}$ and the pressure head

$$\pi = \frac{1}{\rho_0}P + \tfrac{1}{2}|\mathbf{u}|^2$$

where P is the pressure and ρ_0 the reference fluid density. In the above equations ν is the kinematic viscosity, κ the coefficient of thermal diffusivity, α the coefficient of thermal expansion and $\mathbf{g}$ the gravitational acceleration pointing in the negative direction of the z-axis. The fluid is contained between plates positioned at $z = \pm\frac{1}{2}d$ and the boundary conditions for $\mathbf{u}$ are

$$\mathbf{u}(x,y,\pm\tfrac{1}{2}d) = 0 \tag{3}$$

and the boundary conditions for $T(x,y,\pm\frac{1}{2}d)$ are described in the next section. For numerical convenience, we employ periodic boundary conditions in the horizontal directions

$$\mathbf{u}(x+L_x, y+L_y, z) = \mathbf{u}(x,y,z) \tag{4a}$$

$$T(x+L_x, y+L_y, z) = T(x,y,z) \tag{4b}$$

where L_x, L_y are the periodicity lengths. While equations (1a)–(1c) are commonly nondimensionalized to make explicit their dependence on the Rayleigh number $Ra = |\mathbf{g}|\alpha\Delta T d^3/(\kappa\nu)$ and the Prandtl number $Pr = \nu/\kappa$, in our work we have used the dimensional form with values of the fluid properties in SI units corresponding to air, i.e. $\nu = 1.8\times10^{-5}$ m^2 s^{-1}, $\kappa = 2.5\times10^{-5}$ m^2 s^{-1} so that $Pr = 0.71$. The distance d between plates was set to 0.01 m.

The principal quantity of interest in this work is the normalized heat flux (the Nusselt number)

$$Nu = (\langle wT'\rangle - \kappa\,\partial_z\langle T\rangle)/(\kappa\Delta T/d) \tag{5}$$

where $\langle \ldots \rangle$ denotes averaging over horizontal planes and T' denotes departure from the mean $\langle T \rangle$

$$T' = T - \langle T \rangle = T - \left[T_0 - \frac{\Delta T}{d}\left(z - \frac{1}{2}d\right)\right] - \langle \underset{\sim}{T} \rangle.$$

Equations (1a)–(1c) are solved using the pseudo-spectral numerical method as described by Gottlieb *et al.* [13]. In the horizontal directions, the dependent variables are expanded in Fourier series, whereas in the vertical direction, a Chebyshev expansion is employed. Thus, velocity components are represented as follows:

$$\mathbf{u}(x, y, z, t) = \sum_{|k|<K} \sum_{|m|<M} \sum_{n=0}^{N} \mathbf{u}(k, m, n, t) \times \exp\left(-\frac{2\pi i k x}{L_x}\right) \exp\left(-\frac{2\pi i m x}{L_y}\right) T_n(z) \quad (6)$$

with a similar representation for the temperature field. Details of the numerical method and spatial and temporal requirements for accurate simulations are given elsewhere [8].

3. THE NON-UNIFORM TEMPERATURE BOUNDARY CONDITIONS

The simplest numerical method that could be devised to influence heat transfer was through the boundary conditions for temperature at the plates. In the classical Rayleigh–Benard problem, these boundary conditions are

$$\underset{\sim}{T}(x, y, \pm \tfrac{1}{2}d) = 0. \quad (7)$$

In this paper, we use the non-uniform boundary conditions for the temperature at the lower plate in the form

$$\underset{\sim}{T}(x, y, -\tfrac{1}{2}d) = A\Delta T \sin(nk_y y) \quad (8a)$$

and zero boundary conditions at the upper plate

$$\underset{\sim}{T}(x, y, \pm \tfrac{1}{2}d) = 0. \quad (8b)$$

In formula (8a), we take $A = 0.2$, $k_y = 2\pi/L_y$ and n is an integer controlling number of forced convective rolls in the domain of size L_y. For $n = 0$ (or $A = 0$), we get the case of the natural Rayleigh–Benard convection with a temperature difference ΔT between the plates. For $n \neq 0$ the temperature difference is a function of the variable y. In this case, the mean temperature difference, after averaging over horizontal planes, is again ΔT. In both cases, ΔT is used to define the Rayleigh number though for $n \neq 0$ the Rayleigh number should be understood in this averaged sense.

It should be noted that similar sinusoidal temperature perturbations, formula (8a), are used in the stability theory of Rayleigh–Benard convection. Kelly and Pal [14] discuss effects of formula (8a) with $A \ll 1$ and $k_y = k_c$, where k_c is the critical wave number for the onset of convection. They show that the forcing, formula (8a), leads to an imperfect bifurcation in the vicinity of the critical point. Coullet [15] and Coullet and Huerre [16] use similar spatial forcing to describe effects of competition between external and internal length scales in slightly supercritical convection. The main difference between those stability analyses and this work is in the value of parameters used to describe convection and boundary conditions. Stability analysis deals mainly with convective states close to the onset of convection and small amplitudes of forcing in formula (8a). Its advantage lies in the ability to describe phenomena involving large numbers of convective rolls and long evolution times. Direct numerical simulations used in this paper allow analysis of states far removed from the transition point and large amplitudes of forcing in formula (8a). Their limitation is that usually at most a few convective structures may be simulated for necessarily finite times.

Table 1. Maximum Nusselt number for different values of Ra and n

Run	Ra	n	Nu
1	9000	0	2.197
2	9000	2	2.405
3	9000	3	2.689
4	9000	4	2.797
5	9000	5	2.780
6	35840	0	3.37
7	35840	1	3.30
8	35840	2	4.00
9	35840	3	3.46

4. RESULTS OF THREE-DIMENSIONAL SIMULATIONS

Summary of all three-dimensional runs is given in Table 1.

4.1. $Ra = 9000$

It was reported by Willis *et al.* [2] that the characteristic length of the large-scale structures in Rayleigh–Benard convection is a function of Rayleigh number. This length is experimentally measured, averaged horizontal size of two convective rolls (wavelength of convection) which is a relatively well-defined quantity even for three-dimensional flow patterns. According to the experimental results of ref. [2] at $Ra = 9000$ the wavelength of the natural convection is equal to $3.6d$. Our three-dimensional simulations at this Rayleigh number were performed in a computational box with $L_x = L_y = 7.2d$ which is twice the natural wavelength. Boundary conditions (8a) were used with $n = 0, 2, 3, 4$ and 5. All simulations were initialized with a quiescent velocity field and a small random temperature perturbation. Our previous experience [8] and other independent work [5, 17] indicates that convection develops in about two large

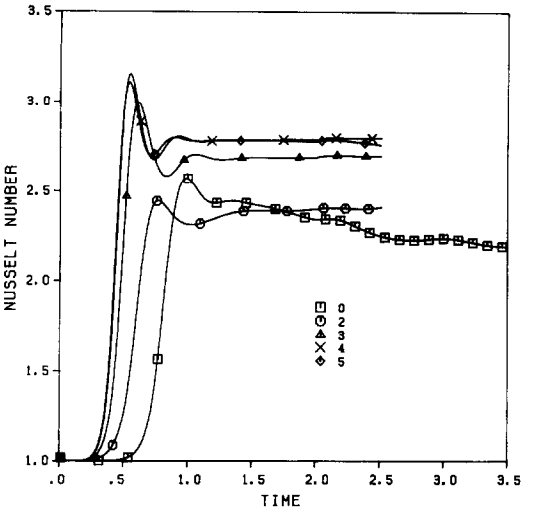

FIG. 1. Nusselt number as a function of time for $Ra = 9000$ and different values of parameter n (marked on the figure).

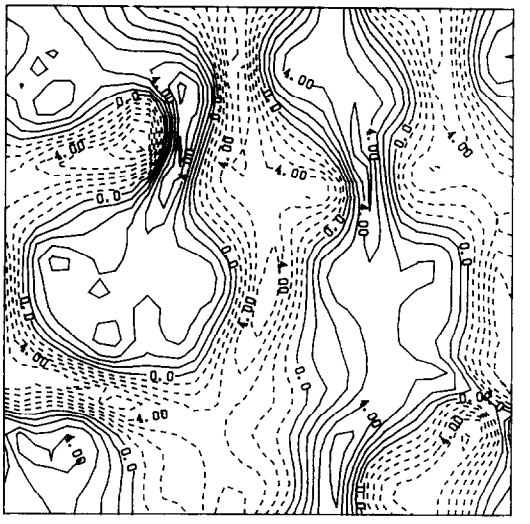

FIG. 2. Contour plot of the vertical velocity w in the plane $z = 0$ for run 1 at $t = 3.5$ (0.875). Here and in the subsequent figures the solid lines correspond to positive values and dotted lines to negative values.

eddy-turnover times, where the eddy-turnover time is defined as

$$\tau \approx \frac{\pi d}{u_{\max}}.$$

Here $u_{\max}$ is the maximum convective velocity. Usually one or two additional large eddy-turnover times are sufficient to achieve quasi-steady state, in which the flow evolution is much slower than in the transition period from the quiescent state to the convective state. For $Ra = 9000$ the eddy-turnover time is $\tau = 0.46$ (0.115). All times in this paper are in seconds followed in parentheses by time in thermal diffusion time units, i.e. $d^2/\kappa = 4$ s. To reach quasi-steady convection, we had to run our simulations for about 1500 time steps when non-uniform temperature boundary conditions were used. With uniform temperature boundary conditions about 2000 time steps were needed to reach quasi-steady state. Spatial resolution was 32×32 horizontal (Fourier) and 33 vertical (Chebyshev) modes. Simulations were performed on a Cray X-MP and required about 2 s per time step.

Figure 1 shows the time evolution of the Nusselt number for runs 1–5. A distinctive feature of the transition period $t < 1.5$ (0.375) is decreasing time for the development of the convection from the quiescent state for increasing n. This time is longest for the case of natural convection ($n = 0$) and decreases for larger values of n until for $n = 4$ and 5 it seems to reach a minimum. Also the time necessary for the Nusselt number to stabilize at an approximately constant value is longest for $n = 0$ and shortest for $n = 4$ and 5. These effects may be explained by the presence of the non-uniform boundary conditions for the temperature which amplify the instability process caused by the random temperature perturbation and by this action accelerate the process of transition to a state of fully developed convection. For $n = 0$ at the end of run 1, the Nusselt number is still evolving but its value, $Nu = 2.197$, is very close to the experimental results ($Nu = 2.167$ [2] and 2.19 [18]) and we do not expect that it would change significantly for later times. When a contour plot of the vertical velocity component in the x–y plane at $z = 0$ for run 1 is examined (Fig. 2), we see that the flow developed two large-scale structures (as expected). However, the convection is far from being purely two-dimensional exhibiting characteristic contractions and expansions of the convective structures. This behavior is very similar to the behavior of convection observed in the simulations of Lipps [5] for $Ra = 9000$, which he attributed to travelling wave disturbances superimposed on convective rolls.

For $n = 2$, the asymptotic value of the Nusselt number is $Nu = 2.405$ and we found that this value was in excellent agreement with the results of two-dimensional simulations that we performed with the same boundary conditions. The agreement between two- and three-dimensional results can be explained by the fact that the convective structures forced by boundary condition (8a) are almost two-dimensional as seen in Fig. 3.

For higher values of n, the Nusselt number increases to a maximum of $Nu = 2.797$ for $n = 4$. A contour plot of the vertical velocity for $m = 4$ shown in Fig. 3(b) indicates that in this case, convection occurs in a form of $2n$ counterrotating, almost two-dimensional rolls. Such a form of convection was observed also for $m = 3$. There is a continuous heat transfer increase for an increasing value of parameter n up to $n = 4$. For $n = 5$ we do not observe any additional heat transfer increase but on the contrary, the Nusselt number starts to decrease at the end of the run and the observed roll pattern exhibits an increase of three-

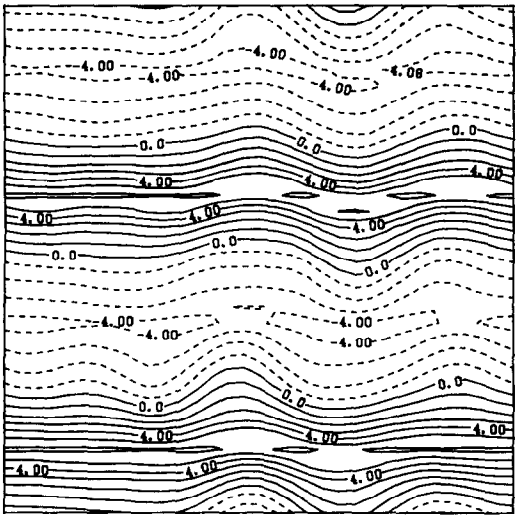

(a)

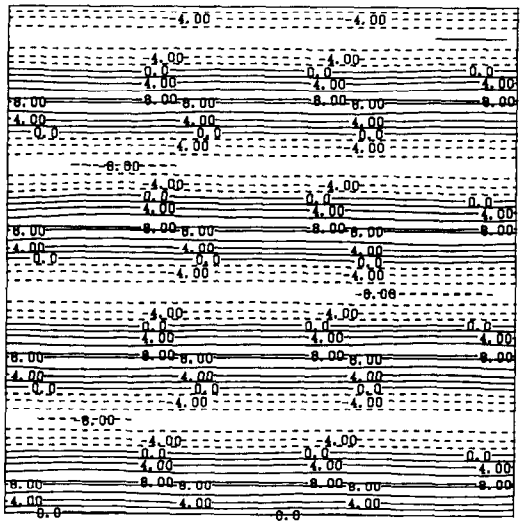

(b)

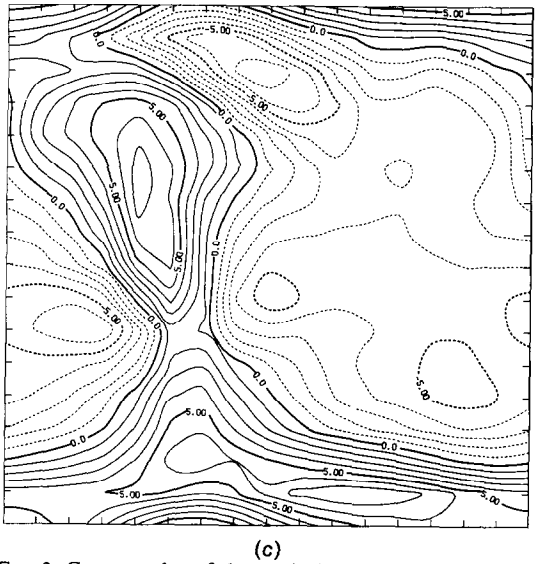

(c)

FIG. 3. Contour plot of the vertical velocity w in the plane $z = 0$: (a) run 2, $t = 2.5$ (0.625); (b) run 4, $t = 2.5$ (0.625); (c) run 4, $t = 12.3$ (3.075).

dimensional effects indicating a possibly unstable situation.

At this point it is important to discuss an effective heat transfer increase that was achieved in our simulations and the question of the stability of forced convective states with wavelengths significantly different from the wavelength of the natural convection.

The effect of boundary condition (8a) with $n \neq 0$ is twofold. It causes the temperature in the fluid to be a function of the horizontal variables and for such a temperature distribution, a mechanical equilibrium is impossible [19]. It was shown by Kelly and Pal [14] that in this case convection occurs even for $Ra < Ra_c = 1707.8$ (the critical Rayleigh number for natural convection), and for $Ra > Ra_c$ properties of the convection with boundary condition (8a) with $n \neq 0$ may be different from the properties of the natural convection at the same Rayleigh number. The second effect of formula (8a) is to impose the wavelength of convective structures that may be different from the natural wavelength at a given Rayleigh number. This possibility of controlling the size of the convective rolls is in fact the main incentive to use boundary conditions (8a). However, if we are interested in the heat transfer control through the control of the size of the rolls it is important to establish how much of the change in the heat transfer may be attributed to the changes in the wavelength of the convective elements and how much is simply a reflection of the fact that the convection with boundary conditions (8a) will always have different properties than the natural convection at the same Rayleigh number. This question was investigated by extending run 4 in such a way that at time $t = 2.5$ (0.625) the forcing, formula (8a), was switched off and the run was continued until $t = 5.0$ (1.25) with uniform temperature boundary conditions. The Nusselt number for this run is shown in Fig. 4(a). Immediately after switching off the forcing the Nusselt number drops from $Nu = 2.797$ to 2.595. This last value is about 18% higher than in run 1. The only major difference between these runs is the wavelength of the convection and for this reason we attribute the heat transfer increase to this factor. The difference between values of the Nusselt number in run 4 for $1.5\ (0.375) < t < 2.5\ (0.625)$ ($Nu = 2.797$) and for $t > 2.5$ (0.625) ($Nu = 2.595$) should be attributed to the use of different temperature boundary conditions. This difference constitutes about 9% of the value of the Nusselt number in run 1. We have also performed another set of two-dimensional simulations at $Ra = 9000$ which confirmed that the effect of the change in boundary conditions (8a) from $n = 0$ to $n \neq 0$ accounted for about a 10% increase in the Nusselt number, the remaining difference being due to the change in the size of the convective elements.

Another important aspect of our simulations is a problem of stability of forced convective patterns. In principle it is difficult to apply stability analysis to the convection at large Rayleigh numbers and large values

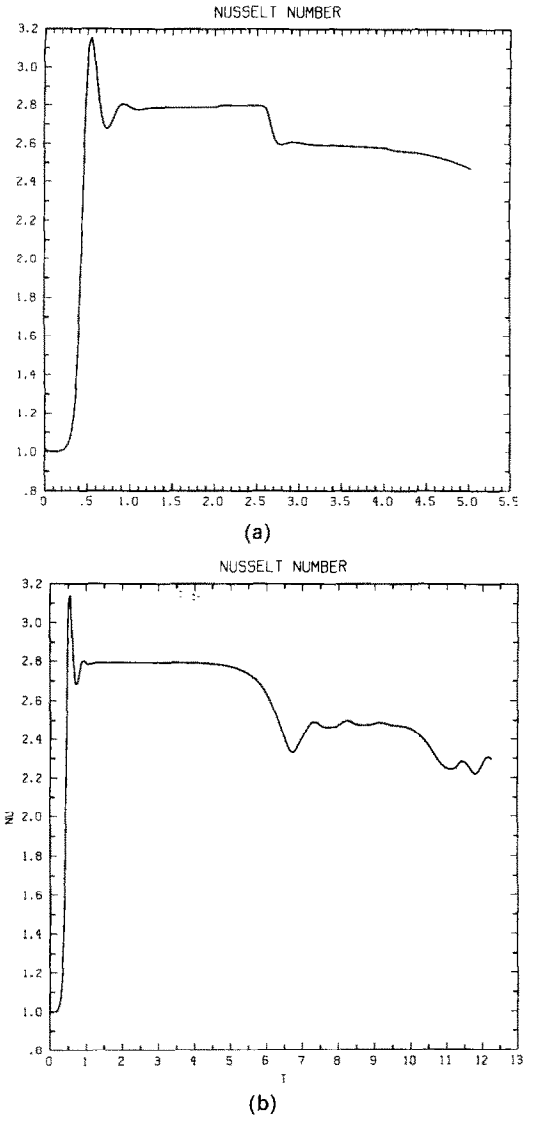

FIG. 4. Nusselt number as a function of time for run 4: (a) forcing switched off at $t = 2.5$ (0.625); (b) long time run with forcing.

of the forcing amplitude A in formula (8a). In direct numerical simulations one may address this problem only by extending simulations to larger spatial domains and integrating equations for longer times. Due to existing limits on computer resources it is especially difficult to assess stability of convective patterns to perturbations with long wavelengths and identify weakly unstable states with decay times much longer than the eddy-turnover time. To investigate this problem more closely we have performed another simulation for the case $n = 4$ that showed the largest increase in the heat transfer. Simulation was run for 25 large eddy-turnover times which is equal to about three vertical diffusion times d^2/κ. The Nusselt number for this run is shown in Fig. 4(b). After initial time $t \approx 1$ (0.25) convection stabilized in a form of four convective rolls (Fig. 3(b)). However, after about ten large eddy-turnover times the Nusselt number experiences a sudden change that is associated with the breakdown of the regular convective pattern into a much less organized form shown in Fig. 3(c). This transition indicates that the forcing through the temperature boundary conditions (8a) is not effective for times longer than about ten large eddy-turnover times.

4.2. $Ra = 35\,840$

Simulations for $Ra = 35\,840$ were performed with $L_x = L_y = 4$ which is also a wavelength of the natural convection at this Rayleigh number [3]. The resolution was again $32^2 \times 33$ modes and simulations were run for about four large eddy-turnover times. The evolution of the Nusselt number for $n = 0$, 1, 2 and 3 is shown in Fig. 5(a). The qualitative behavior of the heat transfer for $Ra = 35\,840$ is the same as for $Ra = 9000$. After a transition period, which becomes shorter for larger values of n, convection reaches a

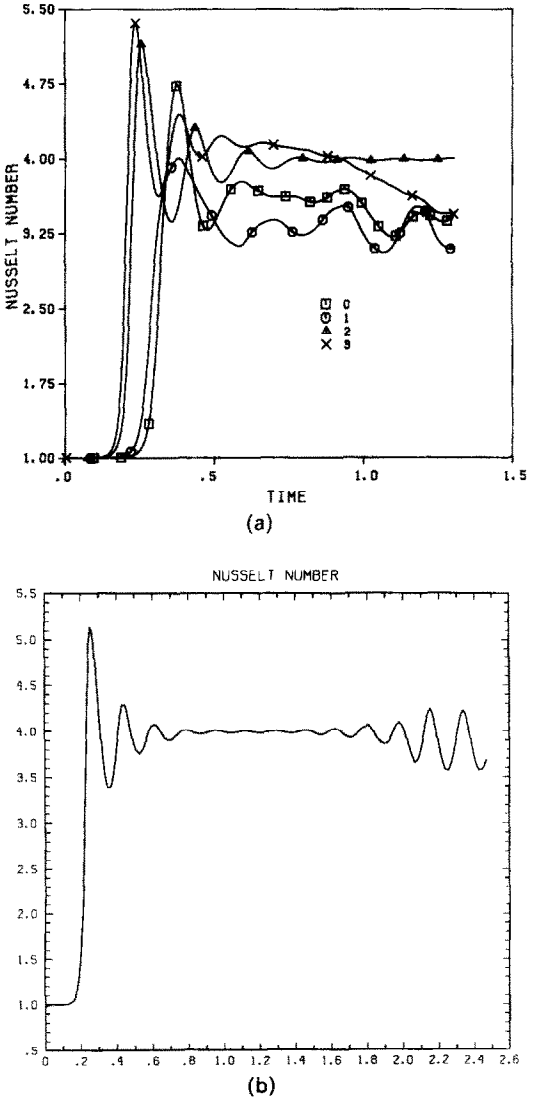

FIG. 5. (a) Nusselt number as a function of time for $Ra = 35\,840$ and different values of parameter n (marked on the figure). (b) Nusselt number as a function of time for run 8.

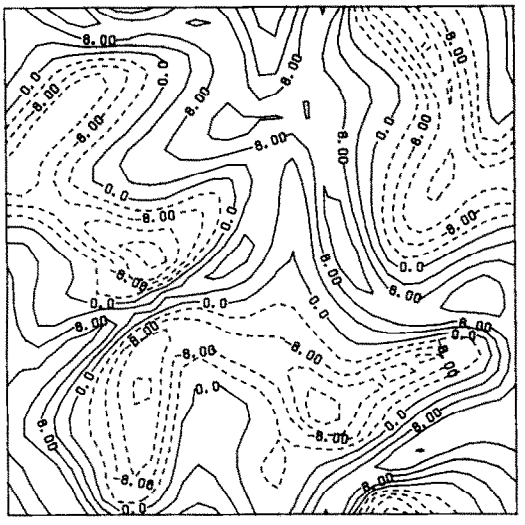

FIG. 6. Contour plot of the vertical velocity w in the plane $z = 0$ for run 6 at $t = 1.3$ (0.325).

quasi-steady state. This time, however, fluctuations of Nusselt number about mean values are relatively large. Such time dependence of the Nusselt number has been reported and discussed in detail by Deardorff and Willis [20] and Domaradzki and Metcalfe [8]. The values of the Nusselt number for $Ra = 35\,840$ given in Table 1 are the mean values at the ends of the respective runs.

A contour plot of the vertical velocity for $n = 0$ (Fig. 6) shows that the convection is highly three-dimensional. Contour plots of the velocity for $n = 1$ at time $t = 1.3$ (0.325) (Fig. 7) show that even with forcing, the convection has a highly three-dimensional appearance. Apparently forcing is ineffective in this case.

Convection in run 8 ($n = 2$) achieves the largest Nusselt number $Nu = 4.00$ and it is well organized in

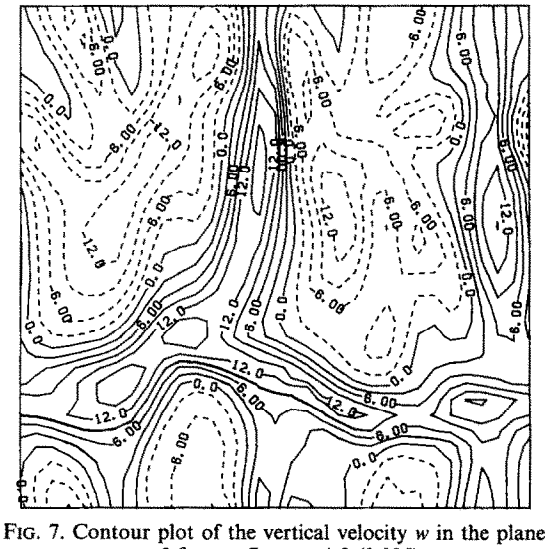

FIG. 7. Contour plot of the vertical velocity w in the plane $z = 0$ for run 7 at $t = 1.3$ (0.325).

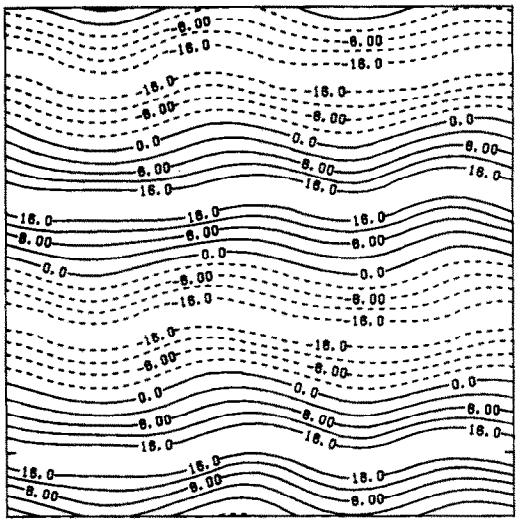

(a)

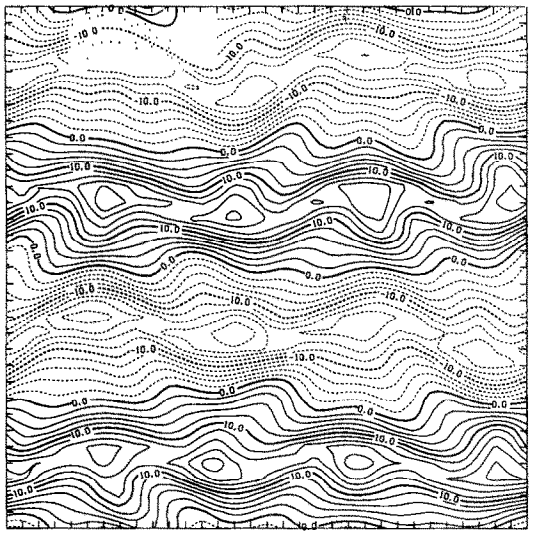

(b)

FIG. 8. Contour plot of the vertical velocity w in the plane $z = 0$ for run 8: (a) $t = 1.3$ (0.325); (b) $t = 2.5$ (0.625).

the form of slightly wavy rolls elongated in the x-direction (Fig. 8). Finally, the convection in run 9 ($n = 3$) is initially excited as three, quasi two-dimensional large-scale structures (Fig. 9(a)) but this form of convection cannot be sustained by the forcing, formula (8a), and the flow experiences transition to a state similar to the case with $n = 0$ (Fig. 9(b)). During this process, the Nusselt number decreases to a value characteristic of the natural convection (Fig. 5(a)). This transition is similar to transition observed for $Ra = 9000$ in the case when $n = 4$. Run 8 which showed the largest increase in the Nusselt number was continued until $t = 2.5$ (0.625) to assess stability of the state with two convective structures in the computational domain for longer times. For $Ra = 35\,840$ the eddy-turnover time is $\tau = 0.22$ (0.055) so that simulations extend for more than ten eddy-turnover

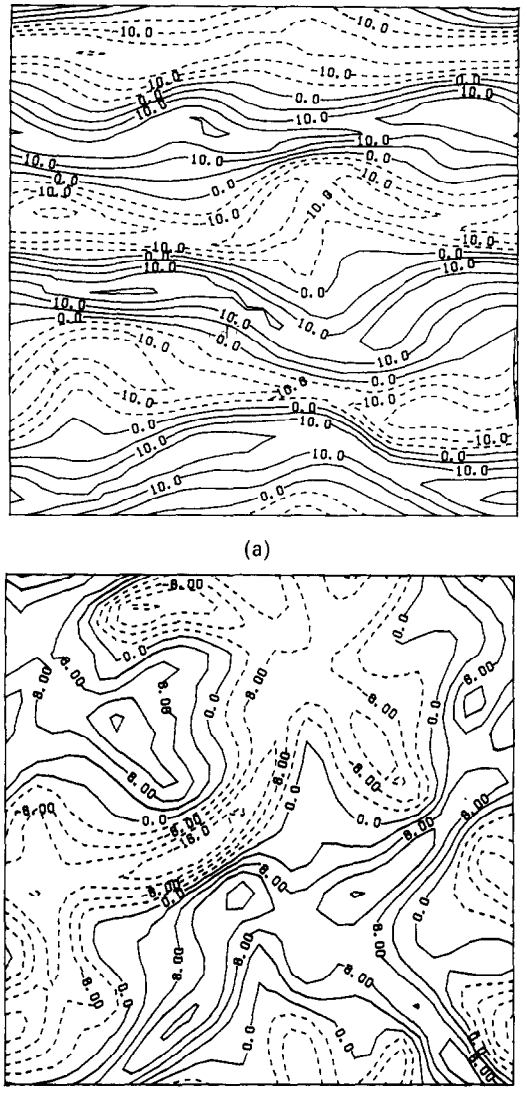

(a)

(b)

FIG. 9. Contour plot of the vertical velocity w in the plane $z = 0$ for run 9: (a) $t = 1.0$ (0.25); (b) $t = 1.3$ (0.325).

times. The Nusselt number for this run is shown in Fig. 5(b). The Nusselt number for $t > 1.5$ (0.375) exhibits increasing oscillations. Such oscillations are seen also in runs 6, 7 and 9 and are expected at this Rayleigh number as discussed in Deardorff and Willis [20] and Domaradzki and Metcalfe [8]. However, the mean Nusselt number does not change in this run for $0.5\ (0.125) \leqslant t \leqslant 2.5\ (0.625)$, i.e. for about ten large eddy-turnover times and the contour plot of the velocity field at $t = 2.5$ (0.625) (Fig. 8(b)) still shows the presence of two large-scale convective structures. Therefore, we conclude that in run 8 the state with two convective structures is stable for at least ten eddy-turnover times. However, based on the results from runs 4 and 9 we may expect that eventually the regular convective pattern in run 8 will also become unstable. The heat transfer increase in run 8 over unforced run 6 is about 20%.

5. CONCLUSIONS

We have shown that with proper forcing, it is possible to control the size of the convective elements in three-dimensional Rayleigh–Benard convection for at least ten eddy-turnover times. The number of large-scale convective structures in a given spatial domain can be two times greater in the convection with forcing than in the natural convection without forcing. If the number of forced convective elements is increased even further, the flow quickly becomes unstable and transitions to the state similar to that of the natural convection. The decrease in the size of the convective rolls and the decrease in a level of three-dimensionality in convection with forcing increases heat transfer by about 15–20%. Even in the best circumstances we observe that the regular, convective patterns forced by the non-uniform temperature boundary conditions (8a) eventually become unstable. It indicates that the forcing chosen in this paper is not effective beyond about ten eddy-turnover times. The forcing through boundary conditions (8a) was chosen because of its relative simplicity in the task of modifying the existing numerical code. However, to stabilize forced convective patterns for longer times it would be interesting to investigate other means of controlling convection. For instance, one may speculate that placing elongated, parallel partitions at the lower plate may force the size of the convective rolls to adjust to the distance between partitions and by this the heat transfer may be increased for long times.

Acknowledgements—The author benefited from discussions with Ralph W. Metcalfe. The numerical program was derived from the FLOGUN code of Steven A. Orszag. This work was supported by the Department of Energy under Contract No. DE-AC06-84ER13153 and the U.S. Office of Naval Research under URIP Contract No. N00014-86-K-0679. Part of this work was performed on computer equipment provided by a grant from the Powell Foundation.

REFERENCES

1. G. E. Willis and J. W. Deardorff, Measurements on the development of thermal turbulence in air between horizontal plates, *Physics Fluids* **8**, 2225–2229 (1965).
2. G. E. Willis, J. W. Deardorff and R. C. J. Somerville, Roll diameter dependence in Rayleigh convection and its effect upon heat flux, *J. Fluid Mech.* **54**, 351–367 (1972).
3. B. J. Daly, A numerical study of turbulence transitions in convective flow, *J. Fluid Mech.* **64**, 129–165 (1974).
4. F. B. Lipps and R. C. J. Somerville, Dynamics of variable wavelength in finite-amplitude Benard convection, *Physics Fluids* **14**, 759–765 (1971).
5. F. B. Lipps, Numerical simulation of three-dimensional Benard convection in air, *J. Fluid Mech.* **75**, 113–148 (1976).
6. G. Grötzbach, Direct numerical simulations of laminar and turbulent Benard convection, *J. Fluid Mech.* **119**, 27–53 (1982).
7. T. M. Eidson, Numerical simulation of the turbulent Rayleigh–Benard problem using subgrid modeling, *J. Fluid Mech.* **158**, 245–268 (1985).
8. J. A. Domaradzki and R. W. Metcalfe, Direct numerical

simulation of the effects of shear on turbulent Rayleigh–Benard convection, *J. Fluid Mech.* **193,** 499–531 (1988).
9. D. A. Hathaway and R. C. J. Somerville, Nonlinear interactions between convection, rotation and flows with vertical shear, *J. Fluid Mech.* **164,** 91–105 (1986).
10. M. M. Chen and J. A. Whitehead, Evolution of two-dimensional periodic Rayleigh convection cells of arbitrary wave-numbers, *J. Fluid Mech.* **31,** 1–15 (1968).
11. F. H. Busse and J. A. Whitehead, Instabilities of convection rolls in a high Prandtl number fluid, *J. Fluid Mech.* **47,** 305–320 (1971).
12. M. Lowe, B. S. Albert and J. P. Gollub, Convective flows with multiple spatial periodicities, *J. Fluid Mech.* **173,** 253–272 (1986).
13. D. Gottlieb, M. Y. Hussaini and S. A. Orszag, *Spectral Methods for Partial Differential Equations* (Edited by R. G. Voigt, D. Gottlieb and M. Y. Hussaini), p. 1. SIAM, Philadelphia (1984).
14. R. E. Kelly and D. Pal, Thermal convection with spatially periodic boundary conditions, *J. Fluid Mech.* **86,** 433–456 (1978).
15. P. Coullet, Commensurate–incommensurate transitions in non-equilibrium systems, *Phys. Rev. Lett.* **56,** 724–727 (1986).
16. P. Coullet and P. Huerre, Resonance and phase solitons in spatially forced thermal convection, *Physica* **23D,** 27–44 (1986).
17. J. B. McLaughlin and S. A. Orszag, Transition from periodic to chaotic thermal convection, *J. Fluid Mech.* **122,** 123–142 (1982).
18. W. Brown, Heat-flux transitions at low Rayleigh number, *J. Fluid Mech.* **60,** 539–559 (1973).
19. L. D. Landau and E. M. Lifshitz, *Fluid Mechanics*, pp. 6–8. Pergamon Press, Oxford (1982).
20. J. W. Deardorff and G. E. Willis, The effect of two-dimensionality on the suppression of thermal turbulence, *J. Fluid Mech.* **23,** 337–353 (1965).

ACCROISSEMENT DU TRANSFERT THERMIQUE DANS LA CONVECTION DE RAYLEIGH–BENARD

Résumé—Des simulation numériques directes de convection 3D de Rayleigh–Benard sont conduites avec des conditions aux limites de température non uniformes sur la plaque inférieure. Les conditions aux limites excitent les états convectifs sous la forme de rouleaux convectifs contrarotatifs qui restent stables pour au moins dix rotations même si leur taille est significativement différente de celle des rouleaux rencontrés en convection naturelle pour le même nombre de Rayleigh. Pour des temps plus longs, les températures appliquées deviennent inefficaces et les configurations de convection forcée perdent leur stabilité. Un changement de la taille des éléments convectifs augmente le transfert thermique de 15–20% environ par rapport au cas de la convection naturelle.

VERBESSERUNG DES WÄRMEÜBERGANGS BEI RAYLEIGH–BÉNARD-KONVEKTION

Zusammenfassung—Die dreidimensionale Rayleigh–Bénard-Konvektion bei inhomogener Temperaturverteilung an der unteren Berandung wurde numerisch berechnet. Die Randbedingungen erzeugen in der Konvektionsströmung gegenläufige Konvektionswalzen, die für mindestens zehn Umlaufzeiten der Wirbel stabil bleiben, obwohl sie sich in der Größe erheblich von den Konvektionswalzen bei reiner natürlicher Konvektion bei derselben Rayleigh-Zahl unterscheiden. Nach längerer Zeit nimmt die Wirksamkeit der Temperaturerhöhung ab, und die Konvektionsströmung verliert ihre Stabilität. Die Änderung der Größe der Konvektionsteilchen vergrößert den Wärmeübergang um 15–20% gegenüber dem Fall der reinen natürlichen Konvektion.

ИНТЕНСИФИКАЦИЯ ТЕПЛОПЕРЕНОСА ПРИ КОНВЕКЦИИ РЭЛЕЯ–БЕНАРА

Аннотация—Выполнено прямое численное моделирование трехмерной конвекции Рэлея–Бенара при неоднородных температурных граничных условиях на нижней пластине. Заданные граничные условия возбуждают противоположно вращающиеся конвективные валы, которые сохраняются приблизительно в течение десяти периодов вращения вихря, даже если их размеры существенно отличаются от размеров валов, образующихся в случае естественной конвекции при таком же значении числа Рэлея. При более длительных промежутках времени влияние неоднородности температуры перестает сказываться и индуцированные конвективные структуры теряют устойчивость. Изменение размера конвективных структур приводит к интенсификации теплопереноса примерно на 15–20% по сравнению с обычной естественной конвекцией.